

# LAGO: A Local-Global Optimization Framework Combining Trust Region Methods and Bayesian Optimization

Eliott Van Dieren<sup>1</sup>, Tommaso Vanzan<sup>2</sup>, and Fabio Nobile<sup>1</sup>

<sup>1</sup>Institut de Mathématiques, École Polytechnique Fédérale de Lausanne, 1015 Lausanne, Switzerland

<sup>2</sup>Dipartimento di Scienze Matematiche, Politecnico di Torino, 10129 Turin, Italy

## Abstract

We introduce LAGO, a **Lo**cal-**G**lobal **O**ptimization algorithm that combines gradient-enhanced Bayesian Optimization (BO) with gradient-based trust region local refinement through an adaptive competition mechanism. At each iteration, global and local optimization strategies independently propose candidate points, and the next evaluation is selected based on predicted improvement. LAGO separates global exploration from local refinement at the proposal level: the BO acquisition function is optimized outside the active trust region, while local function and gradient evaluations are incorporated into the global gradient-enhanced Gaussian process only when they satisfy a lengthscale-based minimum-distance criterion, reducing the risk of numerical instability during the local exploitation. This enables efficient local refinement when reaching promising regions, without sacrificing a global search of the design space. As a result, the method achieves an improved exploration of the full design space compared to standard non-linear local optimization algorithms for smooth functions, while maintaining fast local convergence in regions of interest.

## 1 Introduction

### 1.1 Introduction and motivations

In the past few decades, Bayesian Optimization (BO) (Garnett, 2023; Shahriari et al., 2015) has seen broad adoption in academia and industry as a budget-efficient approach for optimizing expensive black-box functions. Its applications include, among others, hyperparameter tuning for machine learning (Snoek et al., 2012), material design (Mekki-Berrada et al., 2021), and robotics (Berkenkamp et al., 2023). Given a compact set  $\mathcal{X} \subseteq \mathbb{R}^d$ ,  $d \in \mathbb{N}$ , and a continuous function  $f : \mathcal{X} \rightarrow \mathbb{R}$ , BO addresses the problem of finding

$$\mathbf{x}^* \in \arg \min_{\mathbf{x} \in \mathcal{X}} f(\mathbf{x}),$$

by imposing a probabilistic surrogate model over  $f$ , typically a Gaussian Process (GP) (Rasmussen and Williams, 2005), which serves as a prior distribution over functions. The posterior inference is used to improve the knowledge of  $f$  and to guide the selection of the next evaluation of  $f$  through the maximization of an acquisition function, which is designed to be computationally inexpensive to optimize over the design space.

Under regularity assumptions on the function  $f$  and the chosen covariance kernel, BO methods are known to enjoy asymptotic convergence guarantees, typically expressed in terms of sublinear regret bounds or in-fill distance of the search space (Bull, 2011; Srinivas et al., 2012). However, these guarantees are asymptotic and do not prevent repeated sampling in already explored regions which is undesirable under a finite evaluation budget.

While acquisition functions perform well in identifying promising regions, they often induce strong clustering of the evaluation points. Such clustering can lead to near-singular kernel matrices and severe numerical instability in GP inference, particularly for smooth kernels such as the squared exponential one (Wendland, 2004; Wynne et al., 2021).

In practice, the ill-conditioning is mitigated by adding a regularization term (nugget) to the diagonal of the kernel matrix. This regularization improves numerical stability, but alters the GP posterior (Rasmussen and Williams, 2005) and consequently may negatively affect the sequential selection of candidates. Additionally, it also limits the accuracy of the recovered minimum due to the induced regularization floor. As a result, the GP surrogate is generally not an accurate enough model for local optimization.

On the other hand, local gradient-based optimization techniques, such as trust region methods, gradient descent and (quasi)-Newton methods (see, e.g., Nocedal and Wright (2006) for an overview), are designed to efficiently exploit local information and often exhibit fast convergence. However, they are fundamentally limited if the objective function is non-convex, and lack guarantees of global optimality. Even when multiple independent restarts are performed to mitigate the sensitivity to initialization, each run explores only a subset of the design space. Because such restarts are typically treated independently, no information is shared across runs, preventing the reuse of past function evaluations. This results in data-inefficient optimization techniques, which is particularly problematic when function evaluations are expensive, such as in engineering design where function evaluations often entail computationally intensive simulations.

The limitations of both approaches motivate methods that combine the global exploration capabilities of BO with the efficient local exploitation of local optimization techniques.

## 1.2 Contributions

We propose LAGO, a hybrid optimization algorithm that combines gradient-enhanced BO as a global search strategy with gradient-based trust region local optimization centered around the current best solution.

At each iteration, the framework generates both a global candidate from BO and a local candidate from trust region optimization. An adaptive selection mechanism compares their predicted improvements and selects a single evaluation point, ensuring that only one function and gradient evaluation is performed per iteration. A stopping criterion that combines global and local indicators is proposed to terminate the optimization when further improvement is unlikely.

The proposed framework enforces a strict separation between global optimization and local refinement. At each iteration, the BO acquisition function is optimized outside

the active trust region, while local gradient-based optimization is performed inside the trust region. Aside from the trust region center, which is always included in the GP conditioning dataset as the current best minimizer, points close to the trust region center are retained in the GP conditioning dataset only when they satisfy a distance-based criterion relative to the GP lengthscale. This design choice prevents the inclusion of near-identical points that would otherwise induce ill-conditioning of the GP, while retaining critical information about the function landscape within the trust region to guide the BO acquisition function if the trust region is relocated. It also reduces the computational burden of GP inference by keeping fewer points in the conditioning dataset, which typically scales as  $O(n^3)$ , with  $n$  being the number of points in the dataset.

In this work, LAGO is applied to optimization problems with differentiable objective functions. We use gradient-enhanced GPs as global surrogates and quadratic models based on quasi-Newton Hessian approximations within the trust region. Leveraging gradient-enhanced GPs here is natural, as it enables the global surrogate to incorporate derivative information computed during local trust region steps. In many scientific computing problems, gradients can be obtained efficiently via adjoint methods (Plessix, 2006), often at a computational cost comparable to (or smaller than) that of a single (often expensive) function evaluation, making gradient-based optimization particularly attractive. In a machine learning setting, automatic differentiation similarly provides gradients at low additional cost. While gradient-enhanced GPs may limit scalability to moderate dimensions (Rasmussen and Williams, 2005, Section 9.4), LAGO itself is not restricted to gradient-enhanced surrogates and can be instantiated with standard GPs relying solely on function evaluations. Alternatively, in high dimensional problems, derivative information can be included only along a small number of directions (Wu et al., 2017).

### 1.3 Novelty and related works

Hybrid strategies that couple global exploration with local refinement have been extensively studied in the last decades (Diouane et al., 2023; Eriksson et al., 2019; Jones et al., 1993; McLeod et al., 2018; Regis and Shoemaker, 2007). Most approaches typically alternate between local and global phases based on predefined success criteria, such as sufficient decrease conditions, or thresholds on the acquisition function values.

Several methods explicitly combine BO with trust regions, or other local optimization techniques. TREGO (Diouane et al., 2023), for instance, integrates a trust region algorithm with BO, and triggers local steps only when a global step fails to decrease the objective value sufficiently. While effective, this failure-driven switching may delay local refinement, even when a promising local basin has already been identified, and ties local refinement to the inability of the global strategy to improve, rather than to an explicit comparison of local and global improvement potential.

LABCAT (Visser et al., 2025) is another trust region BO technique that relies on rotation alignment of the box trust region based on principal components. The method adaptively discards data points outside the active trust region, which reduces the numerical cost of GP conditioning. However, as noted by the authors, LABCAT is best viewed as a robust local optimization routine rather than a truly global search. Indeed, discarding points outside of the trust region prevents the global overview of the search space.

TuRBO (Eriksson et al., 2019) addresses scalability by maintaining multiple independent trust regions, each equipped with a local GP surrogate. Although effective in high-dimensional settings, this approach fragments the global modeling of the objective function and relies on restarts to reintroduce global exploration. Related extensions (Chen et al., 2025) incorporate Newton-type local solvers but similarly relocate trust regions only intermittently via global acquisition optimization.

BLOSSOM (McLeod et al., 2018) relies on global regret minimization, and combines global BO with local search. It enters the local phase once the regret condition is satisfied and then terminates after local refinement.

BADS (Acerbi and Ma, 2017) combines BO with mesh adaptive direct search (Audet and Dennis Jr, 2006), alternating between local BO searches and global exploration over a discretized mesh based on repeated local failures.

In contrast to these approaches, LAGO considers global and local candidates *simultaneously* at every iteration and selects between them based on predicted improvement. This removes the need for explicit phase switching or failure detection and enables local exploitation as soon as it becomes competitive, including in early stages of the optimization. Moreover, LAGO explicitly decouples local refinement from global exploration. Local trust region steps are not influenced by the global GP surrogate, except for the initialization of the trust region, and are allowed to proceed aggressively without causing ill-conditioning of the global GP, thereby avoiding clustering-induced numerical instability due to the local refinement. At the same time, selective incorporation of local information preserves a coherent global surrogate that continues to guide exploration.

Conceptually, LAGO can then be viewed in two complementary ways: (i) as an enhancement of BO that improves local convergence while reducing the risk of numerical instability due to local refinement, and (ii) as a globalization strategy for classical non-linear optimization, in which the global surrogate guides exploration and enables escapes from suboptimal regions.

## 2 Background

This section describes the two main components used in our algorithm: gradient-enhanced BO (Wu et al., 2017) and the Symmetric rank-one (SR1) trust region method (Nocedal and Wright, 2006).

**Bayesian Optimization.** We first recall the Bayesian optimization framework, and its extension with gradient observations. We model the objective function using a Gaussian Process (Rasmussen and Williams, 2005). This statistical model is attractive due to the availability of closed-form formulas for conditioning. Indeed, conditioning a GP  $\mathcal{GP}(m, k)$ ,  $m : \mathcal{X} \rightarrow \mathbb{R}$  and  $k : \mathcal{X} \times \mathcal{X} \rightarrow \mathbb{R}$  being the prior mean and covariance respectively, on (possibly) noisy observations  $\{(\mathbf{x}_i, y_i)\}_{i=1}^n$ , with  $y_i = f(\mathbf{x}_i) + \xi_i$  and  $\xi_i \sim \mathcal{N}(0, \sigma^2)$ , yields a posterior GP with mean and covariance

$$\begin{aligned}\bar{m}(\mathbf{x}) &:= m(\mathbf{x}) + k_{\mathbf{x}, X}(K + \sigma^2 I_n)^{-1}(\mathbf{y} - m_X), \\ \bar{k}(\mathbf{x}, \mathbf{x}') &:= k(\mathbf{x}, \mathbf{x}') - k_{\mathbf{x}, X}(K + \sigma^2 I_n)^{-1}k_{X, \mathbf{x}'},\end{aligned}$$

where  $m_X = [m(\mathbf{x}_1), \dots, m(\mathbf{x}_n)]^\top$ ,  $K = (k(\mathbf{x}_i, \mathbf{x}_j))_{i,j}$ ,  $k_{\mathbf{x}, X} = [k(\mathbf{x}, \mathbf{x}_1), \dots, k(\mathbf{x}, \mathbf{x}_n)]$  and  $\mathbf{y} = [y_1, \dots, y_n]^\top$ .

One can extend the conditioning of the GP not only on the function evaluations but also on its gradients, resulting in gradient-enhanced GPs (Solak et al., 2002). Instead of modeling  $f$  alone, we leverage the linearity of the gradient operator and place a joint GP prior over  $[f, \nabla f]^\top$  (Rasmussen and Williams, 2005, Section 9.4)

$$\begin{bmatrix} f \\ \nabla f \end{bmatrix} \sim \mathcal{GP} \left( \mathbf{m}_\nabla(\mathbf{x}) := \begin{bmatrix} m(\mathbf{x}) \\ \nabla m(\mathbf{x}) \end{bmatrix}, \quad k_\nabla(\mathbf{x}, \mathbf{x}') := \begin{bmatrix} k(\mathbf{x}, \mathbf{x}') & \nabla_{\mathbf{x}'} k(\mathbf{x}, \mathbf{x}')^\top \\ \nabla_{\mathbf{x}} k(\mathbf{x}, \mathbf{x}') & \nabla_{\mathbf{x}} \nabla_{\mathbf{x}'}^\top k(\mathbf{x}, \mathbf{x}') \end{bmatrix} \right).$$

The posterior distribution of the vector  $[f, \nabla f]^\top$  is again a GP when conditioned on  $\{(\mathbf{x}_i, \mathbf{y}_i^\nabla)\}_{i=1}^n$  with  $\mathbf{y}_i^\nabla = [f(\mathbf{x}_i), \nabla f(\mathbf{x}_i)]^\top + \boldsymbol{\xi}_i$  and  $\boldsymbol{\xi}_i \sim \mathcal{N}(\mathbf{0}, \sigma^2 I_{d+1})$ . The posterior mean and covariance are, respectively,

$$\begin{aligned} \bar{\mathbf{m}}_\nabla(\mathbf{x}) &:= \mathbf{m}_\nabla(\mathbf{x}) + k_{\nabla, \mathbf{x}, X} \tilde{K}_\nabla^{-1} (\mathbf{y}^\nabla - \mathbf{m}_{\nabla, X}), \\ \bar{k}_\nabla(\mathbf{x}, \mathbf{x}') &:= k_\nabla(\mathbf{x}, \mathbf{x}') - k_{\nabla, \mathbf{x}, X} \tilde{K}_\nabla^{-1} k_{\nabla, X, \mathbf{x}'}, \end{aligned}$$

with  $k_{\nabla, \mathbf{x}, X} = [k_\nabla(\mathbf{x}, \mathbf{x}_1), \dots, k_\nabla(\mathbf{x}, \mathbf{x}_n)]$ ,  $\tilde{K}_\nabla := K_\nabla + \sigma^2 I_{n(d+1)}$  and the block-matrix  $K_\nabla := (k_\nabla(\mathbf{x}_i, \mathbf{x}_j))_{i,j}$  is made of  $n \times n$  blocks of size  $d+1$ . We write  $\bar{\mathbf{m}}_f$  for the posterior mean of the function, that is the first element of the vector  $\bar{\mathbf{m}}_\nabla$ . Gradient-enhanced GPs have been used in BO, and yield gradient-enhanced BO (gradBO) (Cheng and Zimmermann, 2023; Wu et al., 2017).

At each iteration of BO (or gradBO), an acquisition function is maximized, and guides the sequential sampling decision. This work focuses on the Expected Improvement (EI) (Jones et al., 1998), and we refer to Frazier (2018) for an overview of alternative choices. The EI is a classical acquisition function that quantifies the expected decrease in value of the objective function if we query it at  $\mathbf{x} \in \mathcal{X}$ . Mathematically, it reads

$$\text{EI}(\mathbf{x}) := \mathbb{E} [(f_{\text{best}} - f(\mathbf{x}))_+],$$

with  $f_{\text{best}}$  being the current best minimum found, and  $(\cdot)_+ := \max(\cdot, 0)$ . The closed form expression using the Gaussian process distribution of  $f \sim \mathcal{GP}(m, k)$  is

$$\text{EI}(\mathbf{x}) = z(\mathbf{x}) \Phi \left( \frac{z(\mathbf{x})}{\sigma(\mathbf{x})} \right) + \sigma(\mathbf{x}) \phi \left( \frac{z(\mathbf{x})}{\sigma(\mathbf{x})} \right), \quad (1)$$

with  $z(\mathbf{x}) = f_{\text{best}} - m(\mathbf{x})$ ,  $\Phi$  and  $\phi$  the standard normal CDF and PDF, respectively. EI therefore solely depends on the GP posterior mean and standard deviation, which are inexpensive to evaluate. As a result, the acquisition function can be optimized at negligible cost compared to the objective function if the latter is expensive to evaluate.

**Trust region algorithm.** The local optimization algorithm used in LAGO consists of a quadratic surrogate model optimization inside a trust region (Nocedal and Wright, 2006). The algorithm places a region around the current best minimizer, and trusts the local quadratic surrogate to approximate the objective function well within that region. The local surrogate is optimized within this region, and the proposed candidate is then accepted or rejected. At iteration  $k$ , given the trust region center  $\mathbf{x}_{k-1}$ , the

method computes a trial step  $\mathbf{s}_k$  and trial point  $\mathbf{x}_k^+ = \mathbf{x}_{k-1} + \mathbf{s}_k$  solving the *trust region subproblem*

$$\mathbf{s}_k \in \underset{\|\mathbf{s}\| \leq \Delta_{k-1}}{\arg \min} m^q(\mathbf{s}), \quad (2)$$

where  $\Delta_{k-1}$  is the trust region radius, and  $m^q : \mathbb{R}^d \rightarrow \mathbb{R}$  is the quadratic model

$$m^q(\mathbf{s}) := f(\mathbf{x}_{k-1}) + \nabla f(\mathbf{x}_{k-1})^\top \mathbf{s} + \frac{1}{2} \mathbf{s}^\top H_{k-1} \mathbf{s},$$

with  $H_{k-1}$  the current approximated Hessian of  $f$ . Theorem 4.1 in Nocedal and Wright (2006) ensures that the trust region subproblem admits a global minimizer. We solve (2) using the standard iterative procedures for trust region subproblems described in Nocedal and Wright (2006, Section 4.3).

To update  $H_{k-1}$  throughout the iterations, we leverage the SR1 update method (Broyden, 1967)

$$H_k = H_{k-1} + \frac{(\mathbf{y}_k - H_{k-1} \mathbf{s}_k)(\mathbf{y}_k - H_{k-1} \mathbf{s}_k)^\top}{(\mathbf{y}_k - H_{k-1} \mathbf{s}_k)^\top \mathbf{s}_k}, \quad (3)$$

where  $\mathbf{y}_k = \nabla f(\mathbf{x}_k^+) - \nabla f(\mathbf{x}_{k-1})$ . This update is done only if

$$|(\mathbf{y}_k - H_{k-1} \mathbf{s}_k)^\top \mathbf{s}_k| \geq r \|\mathbf{s}_k\| \|\mathbf{y}_k - H_{k-1} \mathbf{s}_k\| \quad (4)$$

with  $r \ll 1$ , to avoid numerical instability in (3).

The quality of the trial step is measured by the improvement ratio

$$\rho_k = \frac{f(\mathbf{x}_{k-1}) - f(\mathbf{x}_k^+)}{f(\mathbf{x}_{k-1}) - m^q(\mathbf{s}_k)}, \quad (5)$$

which is then used to decide whether to accept  $\mathbf{x}_k^+$  or not. The SR1 trust region algorithm is given in Algorithm 1, which follows Nocedal and Wright (2006, Algorithm 6.2).

Under the usual assumptions of trust region theory, the trust region algorithm used here guarantees convergence to first-order stationary points, i.e.,

$$\lim_{k \rightarrow \infty} \nabla f(\mathbf{x}_k) = 0,$$

where  $\{\mathbf{x}_k\}_{k \geq 0}$  is the sequence of trust region centers throughout the iterations (see Nocedal and Wright (2006, Theorem 4.6)). Furthermore, for Algorithm 1, under additional regularity assumptions in a neighborhood of a local minimizer  $\mathbf{x}^*$  with  $\nabla^2 f(\mathbf{x}^*) \succ 0$ , the iterates converge superlinearly (Nocedal and Wright, 2006, Theorem 6.7).

### 3 LAGO algorithm description

LAGO relies on the competition between the two optimization routines presented in Section 2: a *global* Bayesian optimization strategy and a *local* trust region method. At each iteration, we follow a selection criterion which adaptively decides whether the local or global step is accepted. The proposed algorithm is currently developed for noise-free objective evaluations, and extending it to noisy settings is a natural direction for future work.

---

**Algorithm 1** SR1 Trust Region algorithm step at iteration  $k$ 

---

- 1: **Input:** Radius  $\Delta_{k-1}$ , Maximum radius  $\Delta_{\max}$ , Acceptance threshold  $\eta \in (0, 0.001)$ , the center  $\mathbf{x}_{k-1}$ .
  - 2: Compute  $\mathbf{s}_k$  solving (2).
  - 3: Define  $\mathbf{x}_k^+ = \mathbf{x}_{k-1} + \mathbf{s}_k$ .
  - 4: Evaluate  $f(\mathbf{x}_k^+)$ , and  $\nabla f(\mathbf{x}_k^+)$ .
  - 5: Compute the improvement ratio  $\rho_k$  with (5).
  - 6: **if**  $\rho_k > \eta$  **then**
  - 7:   (accept)  $\mathbf{x}_k \leftarrow \mathbf{x}_k^+$ .
  - 8: **else**
  - 9:   (reject)  $\mathbf{x}_k \leftarrow \mathbf{x}_{k-1}$ .
  - 10: **end if**
  - 11: **if**  $\rho_k > 0.75$  and  $\|\mathbf{s}_k\| > 0.8\Delta_{k-1}$  **then**
  - 12:    $\Delta_k \leftarrow \min(\Delta_{\max}, 2\Delta_{k-1})$ .
  - 13: **else**
  - 14:   **if**  $\rho_k < 0.1$  **then**
  - 15:      $\Delta_k \leftarrow 0.5\Delta_{k-1}$ .
  - 16:   **else**
  - 17:      $\Delta_k = \Delta_{k-1}$ .
  - 18:   **end if**
  - 19: **end if**
  - 20: **if** (4) holds **then**
  - 21:   Set  $H_k \leftarrow$  SR1 update (3).
  - 22: **else**
  - 23:   Set  $H_k \leftarrow H_{k-1}$ .
  - 24: **end if**
- 

**Global optimization.** The global optimization component is implemented via gradBO. At each iteration, we optimize the acquisition function of choice based on the global gradient-enhanced GP surrogate of the objective function. The acquisition function is optimized *outside* of the trust region. This component ensures global exploration of the search space and mitigates premature convergence to suboptimal regions. Several acquisitions could be used in this setting, and we favor the EI acquisition function in this work, as it is also used in the selection criterion between local and global candidates.

**Local optimization.** We leverage the SR1 method (Algorithm 1) for the local optimization component. The trust region is centered at the current best minimizer  $\mathbf{x}_c$ , and the function and gradient values at this point are used to construct the quadratic surrogate model  $m^q$ . The Hessian of the quadratic surrogate is initialized using the Hessian of the GP posterior mean and updated throughout the local steps using (3). This Hessian does not need to be positive definite, making SR1 updates particularly suited compared, e.g., to BFGS updates (Nocedal and Wright, 2006, Chapter 6.2).

**Selection criterion.** For expensive-to-evaluate functions, we wish to evaluate the function (and its gradient) only once per iteration, similarly to classical BO (Jones et al., 1998). At each iteration, we therefore compare the global and local candidates without evaluating the function at both locations. Let  $\mathbf{x}_G$  and  $\mathbf{x}_L := \mathbf{x}_c + \mathbf{s}_k$  denote the global

and local candidates, respectively. For the global candidate, we compute its expected improvement  $EI(\mathbf{x}_G)$  using (1). For the local candidate, we define the local (deterministic) improvement  $I_t := f_{\text{best}} - m^q(\mathbf{s}_k)$ , where  $f_{\text{best}}$  denotes the objective value at the current trust region center (which always coincides with the current best global minimizer). We select the global candidate if its expected improvement exceeds the predicted local improvement, that is

$$EI(\mathbf{x}_G) > \gamma I_t, \quad (6)$$

with  $\gamma > 0$  a control parameter tuning the local-global behavior of the algorithm. These quantities are both in units of decrease of the cost function, and hence comparable.

Intuitively, selecting the global candidate indicates a higher expected improvement outside the current promising region, whereas selecting the local candidate favors exploiting the current trust region. We note that, since only one function evaluation is permitted per iteration, the selection is based on predicted improvement and does not guarantee the largest realized improvement. Figure 1 shows an iteration of LAGO.

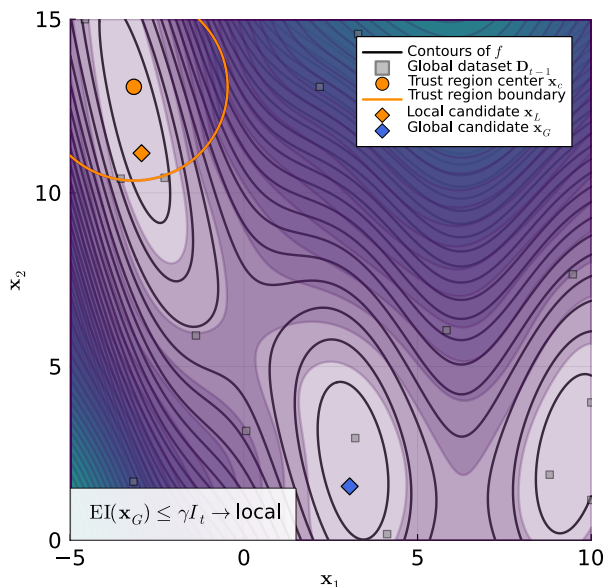


**Figure 1. One LAGO iteration.** The trust region is centered at the current best minimizer. A local candidate is proposed by the SR1 trust region step *inside* the region, while a global candidate is proposed by maximizing  $EI$  *outside* the trust region. Here, the local step will be accepted using (6). Shaded contours show the quadratic surrogate within the region and the GP posterior mean, while the black contours are the true objective values.

**Information flow.** A key feature of LAGO is its one-sided communication from the local to the global component. In particular, updating the global GP does not modify the local optimization routine, except if the trust region is relocated. This preserves the convergence properties of the trust region method, including its superlinear convergence once sufficiently close to a local minimizer. Conversely, to inform the global search about the local landscape within the trust region, we condition the GP on the center of the trust region and on function and gradient evaluations of points that satisfy the

lengthscale-based criterion

$$\{\mathbf{x} \in \mathcal{X} : \|\mathbf{x} - \mathbf{x}_c\|_2 > \nu\ell\}, \tag{7}$$

where  $\ell$  is the GP lengthscale, and  $\nu$  a hyperparameter of choice. In the terminology of scattered data approximation, (7) enforces a lower bound on the separation distance of the design points within the trust region, preventing arbitrarily close samples and thereby mitigating kernel matrix ill-conditioning (Wendland, 2004). Appendix A showcases the necessity of (7) in LAGO to mitigate ill-conditioning.

**Trust region termination.** We require a condition to detect when the trust region procedure has locally converged, in order to update the trust region radius and allow global exploration to continue. Local convergence of the trust region method indicates that no further significant improvement can be obtained within the current trust region, but does not imply global optimality. We check here a step-size condition, declaring the trust region procedure as terminated if  $\|\mathbf{x}_k - \mathbf{x}_{k-1}\| \leq \varepsilon_{\text{step}}$ . When this condition is met, the trust region radius is reset to half the GP lengthscale<sup>1</sup> and the global BO routine is allowed to pursue further exploration of the search space, if necessary.

**Early stopping criterion.** The algorithm terminates early, i.e., before exhausting the allocated evaluation budget, when the following two conditions are *simultaneously* satisfied:

- (C<sub>1</sub>) a sequence of  $N$  global candidates yields acquisition values below a threshold  $\varepsilon_T$ .
- (C<sub>2</sub>) the predicted local improvement  $I_t$  is below  $\varepsilon_T$ .

Condition (C<sub>1</sub>) reflects the absence of meaningful global exploration, while (C<sub>2</sub>) indicates no further predicted local refinement. Only when both conditions are satisfied do we conclude that further improvement by either optimization technique is unlikely.

**Design rationale.** Compared to classical local optimizers, the presence of a global surrogate reduces the risk of stagnation in suboptimal regions, as candidate points are continuously proposed in unexplored or uncertain areas of the search space. By leveraging the accumulated global data to inform the placement of the trust region, LAGO achieves a more data-efficient local refinement than multi-start local methods. Moreover, conditioning the GP on past observations effectively warm-starts the trust region procedure: the quadratic model inherits curvature information from the GP, avoiding repeated reinitializations with an identity Hessian.

Allowing global and local candidates to compete at every iteration ensures that neither exploration nor exploitation is artificially delayed. Local refinement can be activated as soon as it becomes competitive, while the global surrogate continues to monitor the broader search space, maintaining a robust balance between the two regimes throughout the optimization process. The hyperparameter  $\gamma$  provides an intuitive mechanism to tune the local-global trade-off depending on the application at hand. Lastly, Algorithm 2 outlines a comprehensive pseudo-code for LAGO.

---

<sup>1</sup>This choice reduces the risk of the global GP to repeatedly propose candidates near the trust region boundary, which may occur when its radius is too large relative to the GP lengthscale.

---

**Algorithm 2** LAGO: Local-Global BO-TR framework
 

---

- 1: **Input:** objective  $f$ , gradient  $\nabla f$ , design space  $\mathcal{X}$ , acquisition  $\alpha$ , threshold  $\gamma > 0$ , a prior  $\mathcal{GP}(m, k)$ , initial dataset  $\mathbf{D}_0 := \{(\mathbf{x}_i, (f(\mathbf{x}_i), \nabla f(\mathbf{x}_i)))\}_{i=1}^{N_0}$  of size  $N_0$ , initial trust region radius  $\Delta_0$ .
- 2: Obtain the posterior of the GP conditioning on  $\mathbf{D}_0$ , and fit the GP hyperparameters using MLE.
- 3: Compute  $\mathbf{x}^I \leftarrow \arg \min_{\mathbf{x} \in \mathcal{X}} \bar{\mathbf{m}}_f(\mathbf{x})$ , a first informed candidate based on the GP.
- 4:  $\mathbf{D}_1 \leftarrow \mathbf{D}_0 \cup (\mathbf{x}^I, (f(\mathbf{x}^I), \nabla f(\mathbf{x}^I)))$ .
- 5: Initialize the trust region (TR) with center  $\mathbf{x}_c \leftarrow \arg \min_{\mathbf{x} \in \mathbf{D}_1} f(\mathbf{x})$ , radius  $\Delta \leftarrow \Delta_0$  and approximate Hessian  $H$  as the Hessian of the GP posterior mean.
- 6: **for**  $t = 2, 3, \dots$  until the stopping criterion is met **do**
- 7:   **(Optional)** Refit GP hyperparameters (scale and lengthscale  $\ell$ ) periodically.
- 8:   **Global proposal:** Obtain the global candidate

$$\mathbf{x}_G \leftarrow \arg \max_{\mathbf{x} \in \mathcal{X} \setminus B(\mathbf{x}_c, \Delta)} \alpha(\mathbf{x}; \text{GP}).$$

- 9:   **Local proposal:** Get local candidate  $\mathbf{x}_L \leftarrow \mathbf{x}_c + \mathbf{s}_t$  where  $\mathbf{s}_t$  solves (2).
  - 10:   Check whether the TR has terminated.
  - 11:   **if** TR has terminated **then**
  - 12:     Set  $\Delta \leftarrow \frac{1}{2} \ell$ .
  - 13:     Evaluate  $(f(\mathbf{x}_G), \nabla f(\mathbf{x}_G))$ .
  - 14:     Set  $\mathbf{D}_t \leftarrow \mathbf{D}_{t-1} \cup \{(\mathbf{x}_G, (f(\mathbf{x}_G), \nabla f(\mathbf{x}_G)))\}$ .
  - 15:     Condition the GP on  $\mathbf{D}_t$ .
  - 16:     **Continue to next iteration.**
  - 17:   **end if**
  - 18:   Compute the improvement  $I_t \leftarrow f(\mathbf{x}_c) - m^q(\mathbf{s}_t)$ .
  - 19:   **if**  $\text{EI}(\mathbf{x}_G) > \gamma I_t$  **then**
  - 20:     Evaluate  $(f(\mathbf{x}_G), \nabla f(\mathbf{x}_G))$ .
  - 21:     Set  $\mathbf{D}_t \leftarrow \mathbf{D}_{t-1} \cup \{(\mathbf{x}_G, (f(\mathbf{x}_G), \nabla f(\mathbf{x}_G)))\}$ .
  - 22:     Reinitialize the TR if new minimizer found.
  - 23:   **else**
  - 24:     Evaluate  $(f(\mathbf{x}_L), \nabla f(\mathbf{x}_L))$ .
  - 25:     Perform one SR1 trust region step (Algorithm 1) to accept/reject  $\mathbf{x}_L$  and update  $(\mathbf{x}_c, \Delta, H)$ .
  - 26:     **if** new trust region center  $\mathbf{x}_c$  **then**
  - 27:       Set  $\mathbf{D}_t$  by applying (7) to  $\mathbf{D}_{t-1}$ .
  - 28:     **else**
  - 29:        $\mathbf{D}_t \leftarrow \mathbf{D}_{t-1}$ .
  - 30:     **end if**
  - 31:   **end if**
  - 32:   Condition the GP on  $\mathbf{D}_t$ .
  - 33: **end for**
  - 34: **Return:** the best minimizer found  $\mathbf{x}_c$ .
-

## 4 Experimental Results

This section evaluates the empirical performance of LAGO through a convergence comparison with state-of-the-art optimization algorithms on both synthetic benchmark functions and a PDE-constrained optimization problem.

### 4.1 Synthetic tests

We compare LAGO against a representative set of optimization algorithms, including BO (EI) (Jones et al., 1998), gradBO (EI with derivative information) (Wu et al., 2017), BLOSSOM (McLeod et al., 2018), trust region BO variants namely TuRBO with  $M$  regions (TurBO- $M$ ) (Eriksson et al., 2019), TREGO (Diouane et al., 2023) and LABCAT (Visser et al., 2025) with restarts, mesh-based optimization like BADS (Acerbi and Ma, 2017) and local methods such as L-BFGS (Liu and Nocedal, 1989) with restarts. The methods are evaluated on a set of benchmark functions with varying degrees of non-convexity, value range, and multimodality: Branin, Rosenbrock, Levy, Styblinski–Tang (2D and 5D), and Sphere, see Appendix B for definitions. For gradient-based methods, we account for the cost of derivative information by counting one gradient evaluation as equivalent to  $d$  function evaluations, unless stated otherwise.

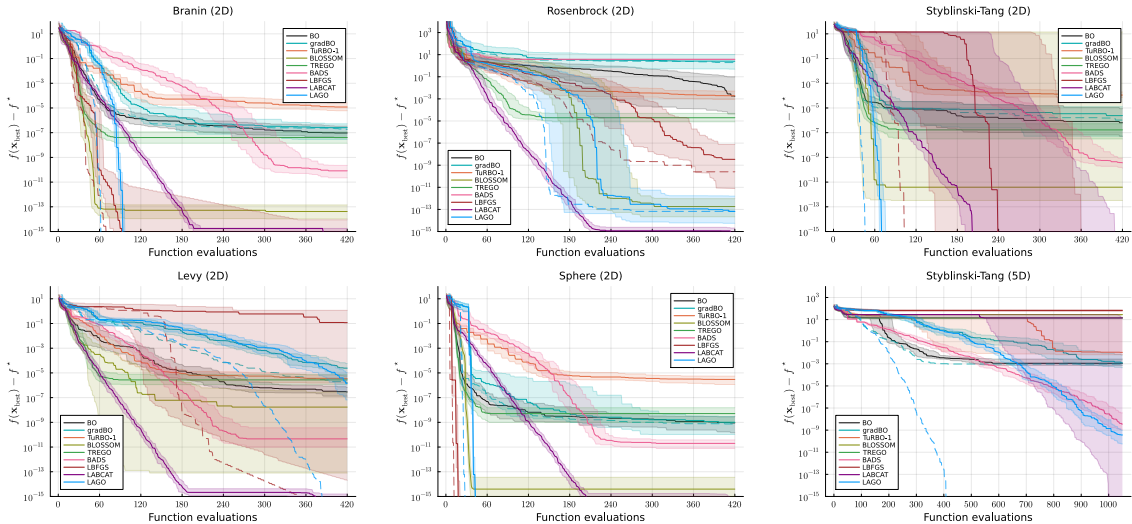


**Figure 2. Synthetic benchmarks.** Comparison of optimization routines over synthetic test functions (Median  $\pm$  IQR as shaded areas). LAGO shows an initial global exploration phase with efficient local refinement once promising regions are identified, and performs consistently well across benchmarks. Local methods such as L-BFGS and LABCAT perform well on convex or near-convex problems, but degrade on multimodal objectives such as Styblinski–Tang, while LAGO remains strong. LAGO performs similarly to BLOSSOM, but outperforms it in higher-dimensions. For gradient-based methods, each iteration is charged a cost equivalent to  $d + 1$  function evaluations; dashed lines indicate the median error in the idealized case in which gradient evaluations have unit cost.

Figure 2 reports the median error (with interquartile range) versus the number of function evaluations across the benchmark problems. LAGO converges reliably across all benchmarks to the global minimum with relatively small variance, reflecting robust performance across runs. In most cases, LAGO initially explores the design space through

its global BO component and subsequently transitions to fast local refinement once a promising region is identified. When a trust region has converged and terminates, the BO component continues to iterate until another region of interest is found, or  $(C_1)$  is satisfied.

On problems where local optimizers consistently converge to the global minimum (e.g., Sphere and Branin), LAGO only has a modest overhead compared to L-BFGS (at most a factor of two in our experiments), primarily due to the gradient-enhanced GP initial training ( $5d$  initial data points).

To explicitly assess robustness to multimodality, we include the Styblinski–Tang function, which features multiple distinct local minima and a unique global minimum. In this setting, local methods such as L-BFGS and LABCAT frequently converge to suboptimal minima, whereas LAGO consistently identifies the global minimum. BLOSSOM also performs competitively on this benchmark but exhibits substantially higher variability. In the 5D instance of this problem, LAGO outperforms all the methods and converges reliably, whereas the performance of local methods degrades in this higher-dimensional non-convex setting.

We further observe that LAGO becomes more sensitive as the objective function becomes ill-conditioned, with Rosenbrock providing a good example for that. Nevertheless, LAGO remains competitive, showing performance comparable to BLOSSOM, and outperforms all the algorithms except LABCAT which performs well in this case and highlights the benefits of incorporating trust region alignment mechanisms combined with local GP conditioning.

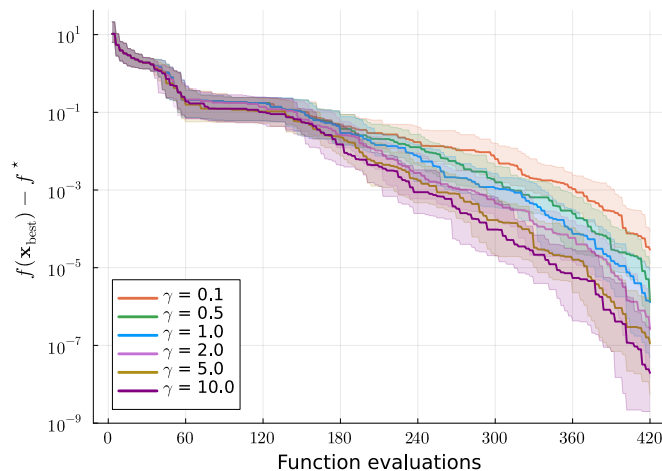


*Figure 3.*  $\gamma$ -ablation. Performance of LAGO on the Levy function for different values of  $\gamma$  in (6) (default  $\gamma = 1$ ). Larger values of  $\gamma$ , which place greater emphasis on local refinement, lead to lower error in this synthetic benchmark.

The Levy function constitutes the most challenging case for LAGO, as its highly multimodal landscape limits the effectiveness of local refinement, and results in a larger proportion of global BO-driven steps. When one gradient evaluation is counted as one function evaluation (dashed line), LAGO is however able to reach the global minimum given the fixed computational budget. We further show in Figure 3 the effect of tuning

the parameter  $\gamma$  in (6) for the Levy function. As  $\gamma$  increases, local refinement is favored over global exploration, and we observe an improvement of the convergence of LAGO as  $\gamma$  grows (default  $\gamma = 1$ ). This also shows the robustness of LAGO with respect to  $\gamma$ .

## 4.2 PDE-constrained optimization

We assess here the performance of LAGO on a PDE-constrained optimization problem (Hinze et al., 2008) for which gradient information can be computed efficiently via adjoint methods.

Let  $\mathcal{D} \subset \mathbb{R}^d$  be a spatial domain. We consider the optimization problem

$$\begin{aligned} \min_{\mathbf{c} \in \mathbb{R}^d} \quad & \tilde{J}(y, \mathbf{c}) := \frac{1}{2} \|y - y_d\|_{L^2(\mathcal{D})}^2 \\ & \text{such that } y \in H_0^1(\mathcal{D}) \text{ satisfies } , \forall v \in H_0^1(\mathcal{D}), \\ & \int_{\mathcal{D}} \kappa(\mathbf{x}) \nabla y(\mathbf{x}) \cdot \nabla v(\mathbf{x}) d\mathbf{x} = \int_{\mathcal{D}} u(\mathbf{x}, \mathbf{c}) v(\mathbf{x}) d\mathbf{x} \end{aligned} \quad (8)$$

where  $u(\mathbf{x}, \mathbf{c}) := \alpha \exp(-\beta \|\mathbf{x} - \mathbf{c}\|_2^2)$  with  $\alpha, \beta > 0$ ,  $\mathbf{c}$  represents the location of the source term,  $y_d : \mathcal{D} \rightarrow \mathbb{R}$  is the desired state, and  $\kappa : \mathcal{D} \rightarrow \mathbb{R}$  is the diffusion coefficient. We define  $J(\mathbf{c}) := \tilde{J}(S(\mathbf{c}), \mathbf{c})$  as the reduced cost function, with  $S : \mathbb{R}^d \rightarrow H_0^1(\mathcal{D})$  being the solution map  $\mathbf{c} \mapsto y(\mathbf{c})$  associated with the PDE constraint. Using the adjoint-state method, the gradient  $\nabla J$  can be computed at the additional cost of solving a single adjoint PDE (Hinze et al., 2008). The adjoint state variable  $p \in H_0^1(\mathcal{D})$  is obtained by solving

$$\int_{\mathcal{D}} \kappa(\mathbf{x}) \nabla p(\mathbf{x}) \cdot \nabla v(\mathbf{x}) d\mathbf{x} = \int_{\mathcal{D}} (y(\mathbf{x}) - y_d(\mathbf{x})) v(\mathbf{x}) d\mathbf{x},$$

$\forall v \in H_0^1(\mathcal{D})$ . Using a Lagrangian approach (see Hinze et al. (2008) for an overview), the gradient reads

$$(\nabla J(\mathbf{c}))_i = - (\nabla_{\mathbf{c}} u(\cdot, \mathbf{c})_i, p)_{L^2(\mathcal{D})},$$

with  $\nabla_{\mathbf{c}} u(\cdot, \mathbf{c}) = 2\alpha\beta \exp(-\beta \|\cdot - \mathbf{c}\|_2^2) (\cdot - \mathbf{c})$ . As a result, evaluating the objective function and its full gradient incurs a cost comparable to two PDE solves, independently of the dimension  $d$  of the control variable. This makes PDE-constrained optimization problems with adjoint-based gradients particularly well suited for LAGO, which explicitly leverages gradient information within its local refinement steps and global gradient-enhanced GP. The details of the PDE-constrained problem are given in Appendix C, where the high multimodality of  $J$  is also illustrated.

Figure 4 shows the convergence of the algorithm when optimizing (8). Local methods with multiple restarts fail to reliably identify the global minimizer and exhibit strong sensitivity to initialization. Global optimization methods perform robustly, but lack the strong convergence speed of the local refinement of LAGO, except BLOSSOM which performs similarly to LAGO.

## 5 Conclusion

We introduced LAGO, a local-global optimization framework that combines Bayesian Optimization with trust-region-based local refinement through an adaptive selection

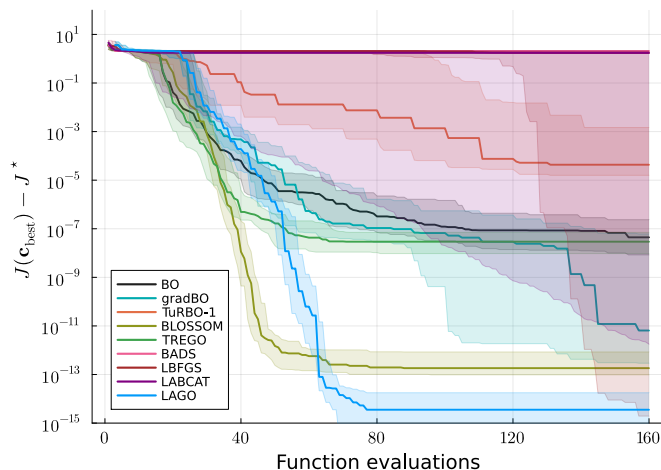


Figure 4. **PDE-constrained optimization.** Comparison of optimization techniques (Median  $\pm$  IQR in shaded areas). By combining global search with gradient-informed local refinement, LAGO achieves excellent convergence in this setting.

algorithm for noise-free differentiable functions. Across a range of synthetic benchmarks and a PDE-constrained optimization problem, LAGO demonstrates strong empirical performance compared to state-of-the-art optimization methods. It is particularly well suited for problems where gradient information can be computed efficiently, such as in PDE-constrained optimization.

By decoupling global exploration from local refinement, LAGO enables fast local convergence in promising regions while reducing the risk of numerical instability during trust region refinement. Overall, these results highlight the benefits of combining global Bayesian Optimization with gradient-based local optimization in a unified framework for smooth, expensive objective functions.

**Limitations.** LAGO is best suited to low- to moderate-dimensional problems, where BO remains effective. While the BO component can accommodate noisy observations, the current trust region refinement assumes noise-free objectives; extending it to noisy settings and high-dimensional problems will be explored in future work.

## References

- Luigi Acerbi and Wei Ji Ma. Practical Bayesian Optimization for Model Fitting with Bayesian Adaptive Direct Search. *Advances in Neural Information Processing Systems*, 30:1834–1844, 2017.
- Charles Audet and John E Dennis Jr. Mesh adaptive direct search algorithms for constrained optimization. *SIAM Journal on optimization*, 17(1):188–217, 2006.
- Felix Berkenkamp, Andreas Krause, and Angela P Schoellig. Bayesian optimization with safety constraints: safe and automatic parameter tuning in robotics. *Machine Learning*, 112(10):3713–3747, 2023.
- Charles G Broyden. Quasi-Newton methods and their application to function minimisation. *Mathematics of Computation*, 21(99):368–381, 1967.

- Adam D. Bull. Convergence Rates of Efficient Global Optimization Algorithms. *Journal of Machine Learning Research*, 12(88):2879–2904, 2011. URL <http://jmlr.org/papers/v12/bull111a.html>.
- Quanlin Chen, Yiyu Chen, Jing Huo, Tianyu Ding, Yang Gao, and Yuetong Chen. Enhancing Trust-Region Bayesian Optimization via Newton Methods. *arXiv preprint arXiv:2508.18423*, 2025.
- Kai Cheng and Ralf Zimmermann. Gradient-enhanced Kriging for high-dimensional Bayesian optimization with linear embedding. *AIAA Journal*, 61(11):4946–4959, 2023.
- Youssef Diouane, Victor Picheny, Rodolphe Le Riche, and Alexandre Scotto Di Perrotolo. TREGO: a trust-region framework for efficient global optimization. *Journal of Global Optimization*, 86(1):1–23, 2023.
- David Eriksson, Michael Pearce, Jacob Gardner, Ryan D Turner, and Matthias Poloczek. Scalable global optimization via local Bayesian optimization. *Advances in Neural Information Processing Systems*, 32, 2019.
- Peter I. Frazier. A tutorial on Bayesian optimization. *arXiv preprint arXiv:1807.02811*, 2018.
- Roman Garnett. *Bayesian optimization*. Cambridge University Press, 2023.
- Nikolaus Hansen, yoshihikoueno, ARF1, Sait Cakmak, Gabi Kadlecová, Guillermo Abad López, Kento Nozawa, Luca Rolshoven, Youhei Akimoto, brieglhostis, and Dima Brockhoff. Cma-es/pycma: r4.4.0, September 2025. URL <https://doi.org/10.5281/zenodo.17167557>.
- Charles R. Harris, K. Jarrod Millman, Stéfan J. van der Walt, Ralf Gommers, Pauli Virtanen, David Cournapeau, Eric Wieser, Julian Taylor, Sebastian Berg, Nathaniel J. Smith, Robert Kern, Matti Picus, Stephan Hoyer, Marten H. van Kerkwijk, Matthew Brett, Allan Haldane, Jaime Fernández del Río, Mark Wiebe, Pearu Peterson, Pierre Gérard-Marchant, Kevin Sheppard, Tyler Reddy, Warren Weckesser, Hameer Abbasi, Christoph Gohlke, and Travis E. Oliphant. Array programming with NumPy. *Nature*, 585(7825):357–362, September 2020. doi: 10.1038/s41586-020-2649-2. URL <https://doi.org/10.1038/s41586-020-2649-2>.
- Michael Hinze, René Pinnau, Michael Ulbrich, and Stefan Ulbrich. *Optimization with PDE constraints*, volume 23. Springer Science & Business Media, 2008.
- Donald R Jones, Cary D Perttunen, and Bruce E Stuckman. Lipschitzian optimization without the Lipschitz constant. *Journal of optimization Theory and Applications*, 79(1):157–181, 1993.
- Donald R Jones, Matthias Schonlau, and William J Welch. Efficient global optimization of expensive black-box functions. *Journal of Global optimization*, 13:455–492, 1998.
- Dong C Liu and Jorge Nocedal. On the limited memory BFGS method for large scale optimization. *Mathematical programming*, 45(1):503–528, 1989.
- M. D. McKay, R. J. Beckman, and W. J. Conover. A comparison of three methods for selecting values of input variables in the analysis of output from a computer code.

- Technometrics*, 21(2):239–245, 1979. ISSN 00401706. URL <http://www.jstor.org/stable/1268522>.
- Mark McLeod, Stephen Roberts, and Michael A Osborne. Optimization, fast and slow: optimally switching between local and Bayesian optimization. In *International Conference on Machine Learning*, pages 3443–3452. PMLR, 2018.
- Flore Mekki-Berrada, Zekun Ren, Tan Huang, Wai Kuan Wong, Fang Zheng, Jiaxun Xie, Isaac Parker Siyu Tian, Senthilnath Jayavelu, Zackaria Mahfoud, Daniil Bash, et al. Two-step machine learning enables optimized nanoparticle synthesis. *npj Computational Materials*, 7(1):55, 2021.
- Patrick Kofod Mogensen and Asbjørn Nilsen Riseth. Optim: A mathematical optimization package for Julia. *Journal of Open Source Software*, 3(24):615, 2018. doi: 10.21105/joss.00615.
- Jorge Nocedal and Stephen J Wright. *Numerical optimization*. Springer, 2006.
- Victor Picheny, Joel Berkeley, Henry B. Moss, Hrvoje Stojic, Uri Granta, Sebastian W. Ober, Artem Artemev, Khurram Ghani, Alexander Goodall, Andrei Paleyes, Sattar Vakili, Sergio Pascual-Diaz, Stratis Markou, Jixiang Qing, Nasrulloh R. B. S Loka, Ivo Couckuyt, and Chris Morter. Trieste: Efficiently Exploring The Depths of Black-box Functions with Tensorflow, 2023. URL <https://arxiv.org/abs/2302.08436>.
- R-E Plessix. A review of the adjoint-state method for computing the gradient of a functional with geophysical applications. *Geophysical Journal International*, 167(2): 495–503, 2006.
- Carl Edward Rasmussen and Christopher K. I. Williams. *Gaussian Processes for Machine Learning*. The MIT Press, 11 2005. ISBN 9780262256834. doi: 10.7551/mitpress/3206.001.0001.
- Rommel G Regis and Christine A Shoemaker. Improved strategies for radial basis function methods for global optimization. *Journal of Global Optimization*, 37(1):113–135, 2007.
- Bobak Shahriari, Kevin Swersky, Ziyu Wang, Ryan P Adams, and Nando De Freitas. Taking the human out of the loop: A review of Bayesian optimization. *Proceedings of the IEEE*, 104(1):148–175, 2015.
- Gurjeet Sangra Singh and Luigi Acerbi. PyBADs: Fast and robust black-box optimization in Python. *Journal of Open Source Software*, 9(94):5694, 2024. doi: 10.21105/joss.05694. URL <https://doi.org/10.21105/joss.05694>.
- Jasper Snoek, Hugo Larochelle, and Ryan P Adams. Practical Bayesian optimization of machine learning algorithms. *Advances in Neural Information Processing Systems*, 25, 2012.
- Ercan Solak, Roderick Murray-Smith, WE Leithead, Douglas Leith, and Carl Rasmussen. Derivative observations in Gaussian process models of dynamic systems. *Advances in Neural Information Processing Systems*, 15, 2002.
- Niranjan Srinivas, Andreas Krause, Sham M. Kakade, and Matthias W. Seeger. Information-Theoretic Regret Bounds for Gaussian Process Optimization in the Ban-

- dit Setting. *IEEE Transactions on Information Theory*, 58(5):3250–3265, 2012. doi: 10.1109/TIT.2011.2182033.
- Elliott Van Dieren and Markus Hauru. evandieren/AbstractBayesOpt.jl: v0.1.3, December 2025. URL <https://doi.org/10.5281/zenodo.18107523>.
- Elliott Van Dieren, Tommaso Vanzan, and Fabio Nobile. Support code for “LAGO: A Local-Global Optimization Framework Combining Trust Region Methods and Bayesian Optimization” v1, March 2026. URL <https://doi.org/10.5281/zenodo.18847398>.
- Emile Visser, Corné E van Daalen, and JC Schoeman. LABCAT: Locally adaptive Bayesian optimization using principal-component-aligned trust regions. *Swarm and Evolutionary Computation*, 97:101986, 2025.
- Holger Wendland. *Scattered Data Approximation*. Cambridge Monographs on Applied and Computational Mathematics. Cambridge University Press, 2004.
- Jian Wu, Matthias Poloczek, Andrew G. Wilson, and Peter I. Frazier. Bayesian optimization with gradients. *Advances in Neural Information Processing Systems*, 30, 2017.
- George Wynne, François-Xavier Briol, and Mark Girolami. Convergence guarantees for Gaussian process means with misspecified likelihoods and smoothness. *Journal of Machine Learning Research*, 22(123):1–40, 2021.

## A Study of the local incorporation condition

In this Appendix, we show the impact of the lengthscale criterion (7) for the incorporation of points nearby the current best minimizer.

Figure 5 reports the median normalized condition number of the global GP kernel matrix around the first occurrence of the local filter introduced in (7), comparing the default setting  $\nu = 0.1$  to the ablation  $\nu = 0$  (no local filter) during the optimization of the Branin function. Across 50 independent runs, we align the iteration count at the first filter activation time  $t^*$  and report the kernel conditioning within a window of  $\pm 3$  iterations (equivalently  $\pm 15$  function evaluations in 2D). A nugget  $\sigma^2 = 10^{-9}$  was added to the diagonal of  $K$ , and we used a Matérn 7/2 kernel. The hyperparameters were tuned every 10 iterations using MLE. We observe that disabling the filter leads to a larger increase in kernel ill-conditioning, consistent with near-duplicate local candidates being incorporated into the global GP training set during trust region refinement. This hence validates the necessity of this local filtering, as proposed in the work.

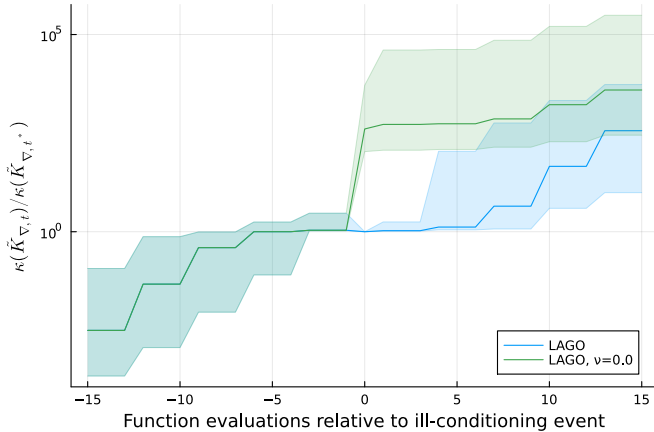


Figure 5. Event-aligned kernel conditioning on Branin (median and IQR (shaded areas) over 50 seeds). We align the iteration count at the first activation  $t^*$  of the local assimilation filter and plot the normalized condition number  $\kappa(\tilde{K}_{\nabla,t})/\kappa(\tilde{K}_{\nabla,t^*})$  within a  $\pm 15$  function evaluations window. Disabling the filter ( $\nu = 0$ ) yields worse conditioning, supporting the role of selective assimilation in improving numerical stability during local trust region refinement.

## B Synthetic experimental framework and algorithm specifications

We discuss here the synthetic problem framework used in Section 4.1. The function definitions, search spaces and the global minima are given in Table 1, while Figure 6 shows the contour plots, with the global minimizers.

We run each algorithm with the same budget of function evaluation ( $210d$ ), over 50 different initial designs of experiments of size  $5d$  using the Latin Hypercube Sampling method (McKay et al., 1979). For gradient-based methods, each iteration is charged a cost equivalent to  $d + 1$  function evaluations, unless stated otherwise. When possible, this initial design is given, but some exceptions apply (see below). If the optimization routine requires only one initial starting point, it is selected randomly from the  $5d$  initial

Table 1. Information about the synthetic test functions used in Figure 2.

Objective	Definition $f : \mathbb{R}^d \rightarrow \mathbb{R}$	Domain	Global minimum
Branin	$(\mathbf{x}_2 - \frac{5.1}{4\pi^2}\mathbf{x}_1^2 + \frac{5}{\pi}\mathbf{x}_1 - 6)^2 + 10(1 - \frac{1}{8\pi})\cos(\mathbf{x}_1) + 10$	$[-5, 10] \times [0, 15]$	0.39789
Styblinski-Tang	$\frac{1}{2} \sum_{i=1}^d (\mathbf{x}_i^4 - 16\mathbf{x}_i^2 + 5\mathbf{x}_i)$	$[-5, 5]^d$	$-39.16599d$
Rosenbrock	$(1 - \mathbf{x}_1)^2 + 100(\mathbf{x}_2 - \mathbf{x}_1^2)^2$	$[-5, 10]^2$	0.0
Levy	$\sin^2(\pi w_1) + (w_1 - 1)^2 [1 + 10 \sin^2(\pi w_1 + 1)]$ $+ (w_2 - 1)^2 [1 + \sin^2(2\pi w_2)]$ , $w_i = 1 + \frac{\mathbf{x}_i - 1}{4}$	$[-10, 10]^2$	0.0
Sphere	$\mathbf{x}_1^2 + \mathbf{x}_2^2$	$[-5.12, 5.12]^2$	0.0

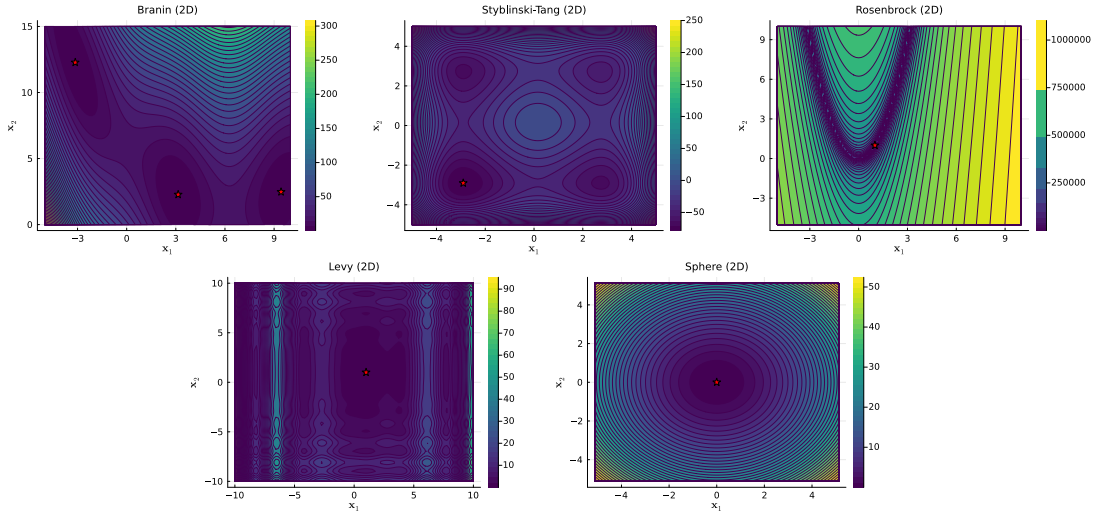


Figure 6. Contour plot of the 2D synthetic test functions. The red stars show the global minima.

data points. If multiple restarts occur, then the next restart point is selected within the remaining points of the initial dataset.

We now discuss the algorithms used for reproducibility purposes. The code to reproduce experiments is available at (Van Dieren et al., 2026).

**LAGO** LAGO was implemented in an in-house Julia library. In our experiments, we set  $\gamma = 1, \nu = 0.1$ , unless stated otherwise. The nugget is set to  $\sigma^2 = 10^{-9}$  and serves as a numerical guarantee for the global GP, the number of acquisition function values needed in Condition (C<sub>1</sub>) is  $N = 5$ , with  $\varepsilon_T = 10^{-12}$ . We set the trust region termination threshold to  $\varepsilon_{\text{step}} = 10^{-7}$ . The kernel chosen throughout the experiments using LAGO is a Matérn 7/2 which is sufficiently smooth to compute the Hessian of the posterior mean, appearing at the initialization of the trust region. We set the prior mean  $m$  to the mean of the function evaluated at the initial data points. The gradient prior mean is zero, by applying the gradient operator to  $m$ . For the MLE hyperparameter tuning of the GP, we leverage the Julia library `AbstractBayesOpt.jl` (Van Dieren and Hauru, 2025), under the version 0.1.3, and train the hyperparameters (lengthscale and magnitude) every 10 iterations. This MLE optimization and prior mean definition are also used for BO and gradBO methods in this work.

The trust region subproblem (2) is solved using a subroutine of `Optim.jl` (Mogensen and Riseth, 2018) (version 1.13.3) implementing the iterative method proposed in Nocedal and Wright (2006, Section 4.3). The SR1 algorithm has been rewritten, and follows

**Algorithm 1.** As for the trust region acceptance, we set  $\eta = 5 \times 10^{-4}$ , and set  $r = 10^{-8}$  in (4).

**BO** Classical BO was used from `AbstractBayesOpt.jl`, under the version 0.1.3. The noise nugget is set to  $\sigma^2 = 10^{-9}$ , and we use a Matérn 5/2 kernel.

**gradBO** Gradient-enhanced BO was also taken from the `AbstractBayesOpt.jl` library, under the version 0.1.3. The noise nugget is set to  $\sigma^2 = 10^{-9}$ , for both the function and its gradient, and we use a Matérn 5/2 kernel.

**L-BFGS** The L-BFGS routine is from `Optim.jl` (1.13.3) with out of the box parameters, and no preconditioners.

**TuRBO** The TuRBO algorithm was taken from the original repository of the authors of [Eriksson et al. \(2019\)](#). TuRBO-5 was also tested but gave similar results to TuRBO-1, and was hence not included in the plots. Two modifications have been made to the original code:

1. For TuRBO-1, we initialize the design of experiments with the same initial design as the other algorithms, but this was not possible for TuRBO-5 where all trust regions have their own initial datasets.
2. The nugget MLE interval has been reduced to  $[10^{-9}; 10^{-8}]$  as we deal with noise-free measurements.

**TREGO** The TREGO routine followed the tutorial provided in the [Trieste \(Picheny et al., 2023\)](#) documentation, as it was also provided as a legitimate source in the original paper ([Diouane et al., 2023](#)). We faced some stability issues with  $\sigma^2 = 10^{-9}$ , which we increased to  $10^{-7}$  for all test cases. For TREGO, numerical instabilities were observed on the Rosenbrock and Sphere function despite tuning the nugget parameter; results for these cases have seen their nugget increased until success ( $\sigma^2 = 10^{-3}$ ).

**LABCAT** The LABCAT algorithm was taken from the repository of the authors of [Visser et al. \(2025\)](#), using the Python interface. The initialization step prevents us to provide an original dataset using the Python framework. We therefore left the original dataset being initialized using a Latin Hypercube Sampling scheme as prescribed in the original paper ([Visser et al., 2025](#)). As a stopping criterion, we put a tolerance on the range of output values of  $10^{-12}$ . If this stopping criterion is met, we restart the optimization loop with the remaining budget, until exhausted.

**CMA-ES** The CMA-ES is using the `pycma` ([Hansen et al., 2025](#)) package with the population  $\lambda = 4 + \lfloor 3 \log d \rfloor$ . We however observed poor performance due to the tight function evaluation constraints, and the method was hence not added to the convergence figures. We however provide the code to run the experiment in the supplementary material for completeness.

**BADS** BADS is using the `pybads` ([Singh and Acerbi, 2024](#)) package.

**BLOSSOM** BLOSSOM was taken from the repository of the authors of [McLeod et al. \(2018\)](#), and the global regret threshold was set to 0.1, as it was seen as the best performing in [McLeod et al. \(2018\)](#) on the synthetic benchmarks.

**Julia-Python interface** LAGO, BO, gradBO and L-BFGS scripts were written and run in Julia 1.12.2. The remaining algorithms were run in Python 3.11.5, except for BLOSSOM which was run on a Python 3.6.13 instance, due to the requirement restrictions of the authors of [McLeod et al. \(2018\)](#). All evaluated points and objective values were stored in NumPy arrays ([Harris et al., 2020](#)) and imported into Julia for post-processing and visualization.

All experiments were run with fixed random seeds, and the DOE were shared and initialized with a master seed.

## C PDE-constrained optimization problem specification

In this section, we introduce the different parameters and functions used to produce the result in Section 4.2. As  $J$  is very smooth, we decided to use a Matérn 7/2 kernel whenever possible (BO, gradBO and LAGO).

**Finite Element Method framework.** For this study, we meshed the physical domain  $\mathcal{D} := [0, 1]^2$  with  $50 \times 50$  squares, further split into two to obtain triangular elements, and used  $P^1$  finite elements.

**Functions used in the system.** The diffusion coefficient is given as

$$\kappa(\mathbf{x}) = \exp(\exp(-1.125)(\cos(\pi \mathbf{x}_1) \sin(\pi \mathbf{x}_2) + \cos(2\pi \mathbf{x}_1) \sin(\pi \mathbf{x}_2) + \cos(2\pi \mathbf{x}_1) \sin(2\pi \mathbf{x}_2))),$$

the desired state  $y_d$  is

$$y_d(\mathbf{x}) := \exp(2\mathbf{x}_1 + 2\mathbf{x}_2) \sin(4\pi \mathbf{x}_1) \sin(4\pi \mathbf{x}_2),$$

and for the source term  $u$  we set  $\alpha = 5 \times 10^2$  and  $\beta = 5 \times 10^3$ .

The landscape of the cost function of (8) is given in Figure 7, which illustrate the presence of local minima and a global minimum located near the top-right of the search domain. All the quantities described above are shown in Figure 8, as well as the obtained state variable  $y$  when we place the source term at  $\mathbf{c}^* \approx (0.89, 0.89)$ .

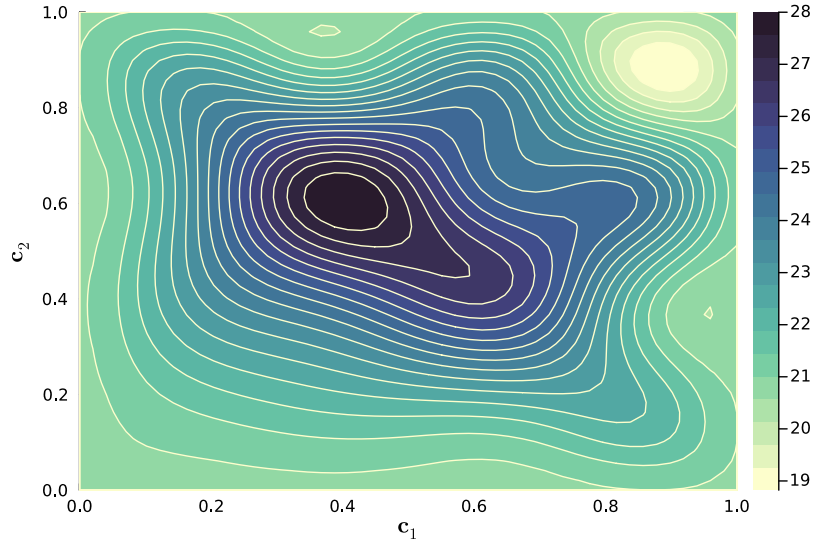


Figure 7. Landscape of the reduced cost function  $J$  for the PDE-constrained optimization problem. The objective exhibits multiple local minima and a distinct global minimizer, highlighting the need for global exploration combined with local refinement.

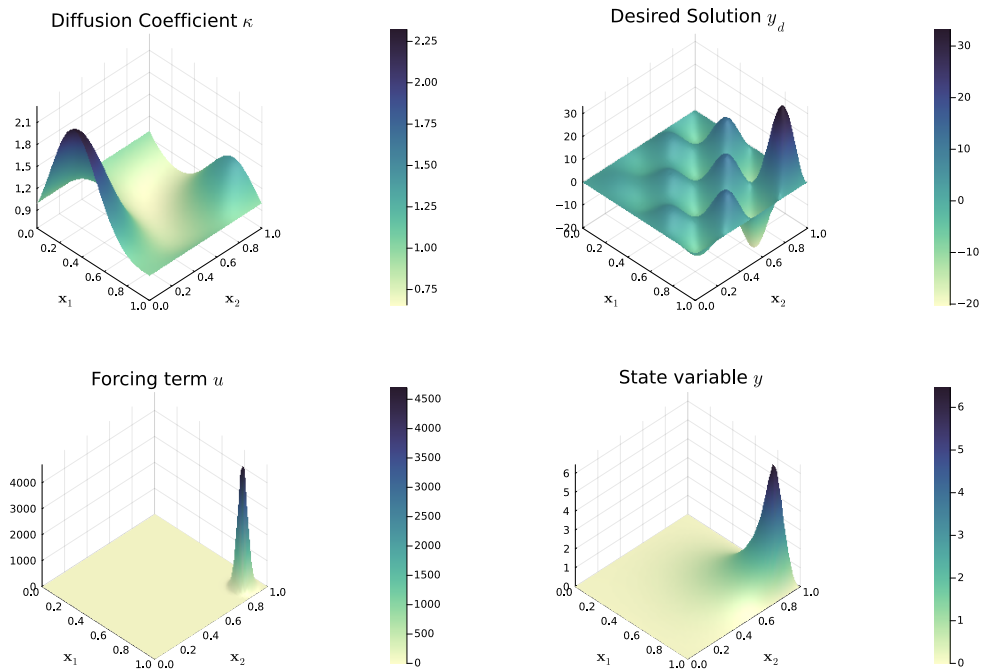


Figure 8. Diffusion coefficient  $\kappa$ , desired state  $y_d$ , optimal forcing term  $u$ , and obtained state variable  $y$ . The forcing term is approximately placed at the highest point of the desired state  $y_d$ , as the resulting state  $y$  will minimize the  $L_2$  error with  $y_d$ .